Parametric Model of an Air-core Measuring Transformer

Dejana Herceg[*,1]
[1]Faculty of Technical Sciences
*FTN, Trg Dositeja Obradovica 6, 21000 Novi Sad, Serbia, vuletic@uns.ac.rs

Abstract: Power grid voltages and currents may be distorted due to presence of harmonics. Measurements of such voltage with harmonics may be performed using newly developed instrument with a small air-core transformer based probe as the input unit. The probe must be shielded against unknown external electromagnetic fields. At the same time, the probe must remain linear throughout the range of frequencies. An air-core transformer based probe was designed with a ferromagnetic shield. A parametric model of the shielded transformer is analyzed. Results obtained from a FEM simulations of the model, as well as options for optimization of the shield are presented.

Keywords: air-core transformer, shielding

1. Introduction

Power quality is a major concern nowadays. This work is a part of a bigger study aimed at power quality improvement. Due to many possible disturbances in a power system, industrial current and voltage may have substantial amount of higher order harmonics on top of the fundamental harmonic of 50Hz. International standards limit harmonic distortion and content [1, 2]. However, the compliance with standards is not easy to verify.

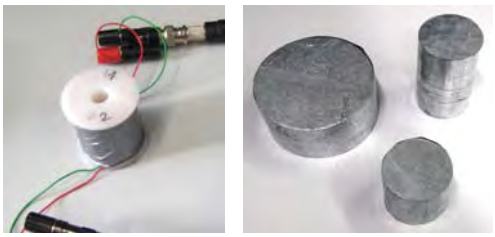

Figure 1. The air-core transformer (left) and the different shields

Harmonic rich voltage measurements may be performed using a small air core transformer based probe as input unit [3, 4]. Such a probe, show in Fig. 1, is the object of this investigation. The goal of this work was to design a shield around the probe in order to protect it from impact of external magnetic field. Once the ferromagnetic shield was chosen, the goal of the research was

- to optimize the shield shape in such a way to cancel the impact of external magnetic field as much as possible, and
- to minimize the influence of the shield on the probe readings.

In order to optimize the shield shape (as the first task), the shielding effectiveness was evaluated. On the other hand, the inductance of the probe was explored because the probe readings were substantially affected by the shield. Also, an increased inductance may filter out the higher harmonics i.e. the inductance of the probe must be kept low, in order not to block the higher harmonics.

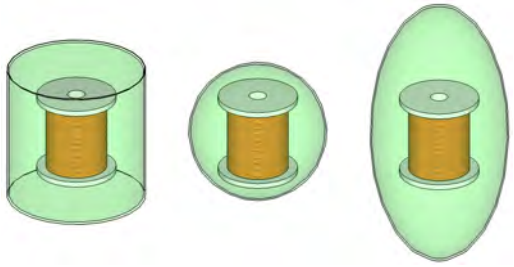

Figure 2. Model of the shielded probe

As well known from the literature, for protection of a small object, the best ferromagnetic shield can be made as a spherical shell [5]. But, a spherical shield may be difficult and expensive to manufacture. For that reason other shapes were considered too:

- cylindrical,
- spherical and
- ellipsoidal.

Different dimensions were considered in order to find the best solution. The probe was centered inside the shields as seen from Fig. 2.

The shield should be made of low cost material. One of the available low-cost ferromagnetic materials with relative permeability of 550 was provided by a local manufacturer. For calculation purposes, relative

permeability of the ferromagnetic material was taken to be 550 and 5500, with conductance of 1.12 10^7S/m. The thickness of the shields were 0.5mm or 5mm. These values were used in calculations, unless stated otherwise.

The influence of the shields was explored numerically, using the finite element method based software COMSOL Multiphysics.

2. Parametric model approach

Optimization of the shields is often performed by varying the parameterized dimensions of the model geometry and performing numerical simulations in order to observe the results for each distinct set of the parameters.

Several ways to create a parametric model were employed here

- geometric parametric sweeps option in COMSOL Multiphysics v3.5a, in connections with a specialized CAD software, such as SolidWorks and AutoDesk Inventor,
- moving mesh (ALE model)
- programming in MATLAB.

The third approach was chosen as it allows varying geometric dimensions without changing the model topology in numerical simulations. COMSOL can be used either through a graphical user interface (GUI) or by executing the COMSOL functions from a MATLAB script, or both.

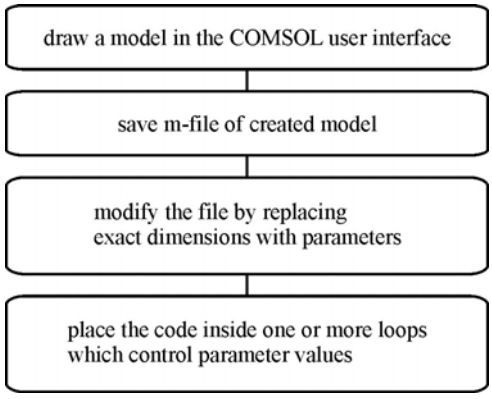

Figure 3. Phases in the parametric model approach

Basic steps in creating parametric model of the probe are presented in Fig. 3. The COMSOL GUI was used to design the probe model and to automatically generate the MATLAB code (.m file) which describes the model. Generated code is then modified by replacing the exact values with parameter variables. After this modification, the resulting code is enclosed in several loops in order to create models for each distinct set of parameters. Alternatively, without using the COMSOL GUI, MATLAB can be used directly to create a script and just run the simulation through loops, although this can be more difficult to execute. In this case COMSOL is used only as a standalone FEM package.

The probe model was built in COMSOL for 2D axisymmetric case with the Azimuthal Induction Currents, Vector Potential application mode, using the time-harmonic formulation. The dependent variable in this application mode is the azimuthal component of the magnetic vector potential.

3. Electromotive force calculation

Starting with Maxwell's equations in time-harmonic case for 2D axisymmetric problems, the azimuthal complex magnetic vector potential, A_φ, obeys the equation

$$\left(j\omega\sigma - \omega\varepsilon_0\varepsilon_r\right)A_\varphi + \nabla\times\left(\frac{1}{\mu_0\mu_r}\nabla\times A_\varphi\right) = J_\varphi ,$$

where ω denotes the angular frequency, σ the conductivity, μ the permeability, and ε the permittivity. J_φ is an external current density imposed in conductor regions and it is also parallel to A_φ.

The complex induced electric field vector can be defined as

$$E_{ind} = -j\omega A_\varphi .$$

Complex induced electromotive force in one turn of the secondary coil is

$$EMF_{turn} = E_{ind}\,2\pi r ,$$

where *r* denotes the radius of the coil.

4. Transformer based probe model

This section contains the description of the dimensions of the model being solved in the current study. The probe consists of an air core transformer with two coils having a large number of turns. The primary coil has 1200 turns of copper wire, 0.2mm in diameter. The secondary coil is wrapped on the top of the primary coil

with the same wire and equal number of turns. The cross-section of the transformer and the shield is shown in Fig. 4. The height of the transformer coils was 40 mm and the inner diameter of the primary coil was 30 mm. Permeability and permittivity of the plastic core were equal to the free space values. The height of the cylindrical core was 46 mm and the diameter was 44 mm.

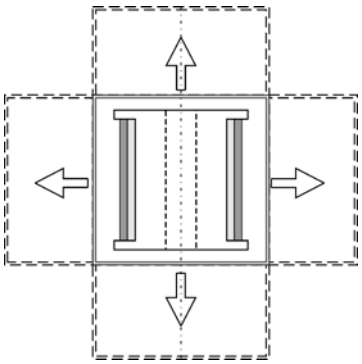

Figure 4. Cross-section of the shielded transformer. The size of the shield varies in simulations

Properties of the shields were defined above. The dimensions of the shield were limited because of the space available. The simulations started with the smallest applicable shields for the three different shapes from Fig. 2: spherical, ellipsoidal and cylindrical. Radius of the spherical shield was varied in the range between 38 mm and 57 mm. For the cylindrical shields, the radius was in the range between 28.5 mm and 85.5 mm and the height was 56 mm or higher, but not larger than 4 times the radius.

The radius of the shield is denoted by *R*, the height by *H*, and the thickness by *d*.

An attenuated signal should be brought to the input of the probe. In the simulations, the primary sinusoidal current was taken to be 1mA (rms value) at each frequency in the range, starting with 50 Hz, up to the 50^{th} harmonic.

The homogeneous external magnetic field was created by a single large diameter (1m) current loop, as demanded by the standard [6]. A 50 Hz magnetic field, with a rms value of 100A/m, was applied as an external disturbance.

5. Results and discussion

Fig. 1 shows magnetic flux density calculated for the unshielded transformer when a sinusoidal current of 1 mA and 50 Hz was applied to the primary. This is a well known magnetic field distribution of the solenoid.

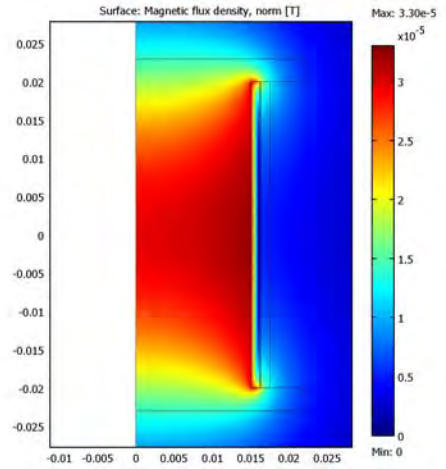

Figure 5. Magnetic flux density inside the coils of the unshielded transformer; primary current applied.

In Fig. 6, one can observe the magnetic field distribution inside and outside of the shield, when an external magnetic 50 Hz field is present. Inside the coils, the value of the magnetic field was 20A/m and this value was 5 times less than without the shield.

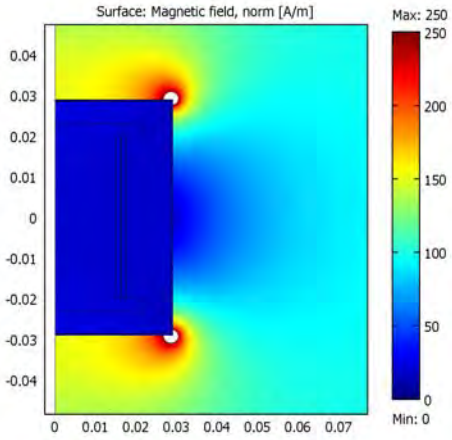

Figure 6. When the external magnetic field is present, the magnetic field inside the coils is around 20A/m; 5 times less than without the shield. (R=28.5mm, H=2R, d=0.5mm)

In order to compare the impact of the external magnetic field to the transformer with different shield shapes, the shielding efficiency was calculated. The shielding efficiency is defined as

$$S_e = \frac{B_0}{B_{sh}} = \frac{EMF_0}{EMF}.$$

where B_0 and B_{sh} denote the magnetic flux density before and after the shield is applied, respectively. EMF_0 and EMF represent the electromotive force on the secondary coil of the unshielded and shielded transformer, respectively.

To check the accuracy of the formulas and methods, the spherical shield was investigated first. For a small spherical high permeability ferromagnetic shell in a homogeneous time varying field, shielding effectiveness can be calculated analytically as explained in [7]. Analytical value for the shielding efficiency for the smallest applicable radius R=38mm, thickness d=0.5mm and relative permeability μ_r=550 is 5.8. In FEM simulations this value was calculated to be 5.76 (Fig. 7).

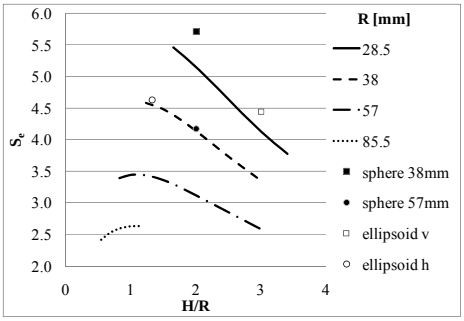

Figure 7. Shielding efficiency as a function of H/R ratio for different shield shapes (0.5mm shield thickness).

Shielding efficiency for the two different thickness values (0.5mm and 5mm) are shown in Figs. 7 and 8. Black points denote values for the spherical shields, white points for the ellipsoidal shields and the lines for the cylindrical shields. For the ellipsoidal shields equatorial and polar diameters were 76 mm and 114 mm ("v" stands for vertical orientation and "h" for horizontal). The spherical shield shape seems best, but difficult to manufacture. Smaller cylindrical shields (represented by full and dashed lines) can be a good solution too. If the Figs. 7 and 8 are compared, thicker shields provide a better S_e. On the other hand, thicker shields affect the linearity of the transformer more. For μ_r=5500, S_e is approximately 10 times higher than for μ_r=550.

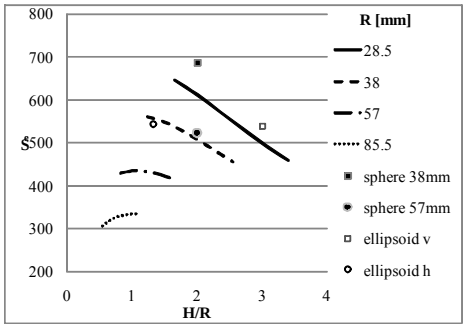

Figure 8. Shielding efficiency as a function of H/R ratio for the different shield shapes with 5mm thickness

Impact of the shield on the induced *EMF* on the secondary coil can be expressed by a new quantity-the transformer linearity coefficient. This coefficient was defined as

$$k = \frac{EMF}{freq},$$

where *EMF* stands for the induced electromotive force on the secondary and *freq* for the frequency of the input signal on the primary. The normalized transformer linearity coefficient is

$$k_N = \frac{EMF}{EMF_0} = \frac{L}{L_0},$$

where L and L_0 denote inductance before and after the shield is applied, respectively.

Theoretically, the transformer linearity coefficient for the unshielded case is constant and equals

$$k_0 = \frac{EMF_0}{freq} = 0.1553 \text{ mV/Hz}.$$

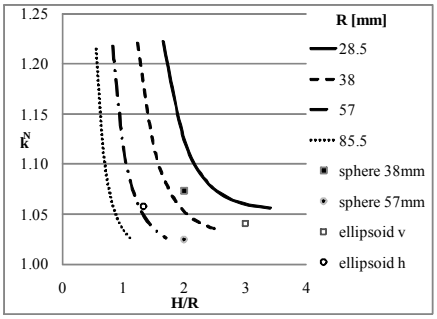

Figure 9. Normalized coefficient k_N as a function of the H/R ratio for the different shield shapes with the same d=0.5mm and μ_r=550 for all shields

Fig. 9 shows the impact of the shield shape on induced EMF on the secondary coil. In the

ideal case, k_N is equal 1 (no impact of shied). Meaning of the dots and lines in Fig. 9 is the same as in Figs. 7 and 8. The impact of the shield, expressed by the coefficient k_N, and the size of the shield are inversely proportional. Lower k_N values are better. The best shield in this case is the larger sphere, but the cylinder with R=38 mm also performs well.

All calculated results up to this point were calculated for a basic frequency of 50Hz. From this point on, the transformer linearity coefficient *k*, will be discussed as function of the frequency in the range from 50 Hz up to 2500 Hz. A constant value of *k* is desirable throughout the whole range of the frequencies.

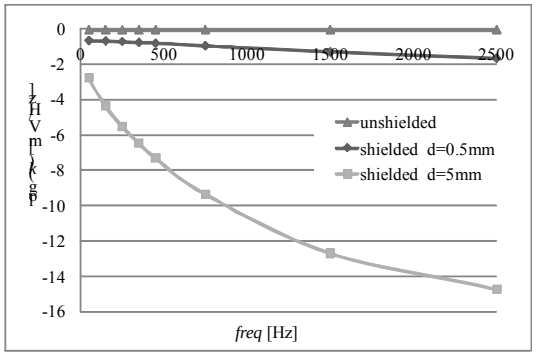

Figure 10. Impact of the external magnetic field is expressed by the transformer linearity coefficient as function of magnetic field frequency.

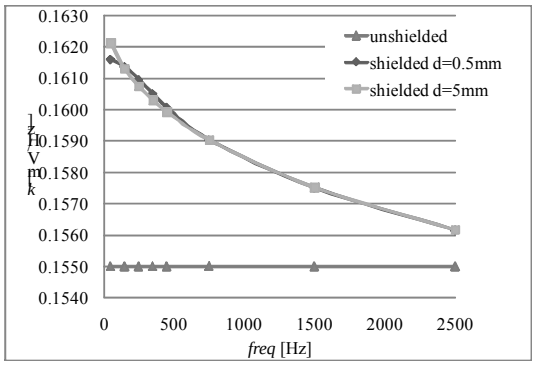

Figure 11. Shield shape influence on the transformer linearity coefficient as a function of the frequency of the input signal on primary winding.

Fig. 10 shows the transformer linearity coefficient as function of magnetic field frequency when the external magnetic field is present. One can observe that for the thinner shields, better values of the linearity coefficient are obtained. The transformer ratio is directly proportional to the coefficient *k* and does not stay the same for all frequencies, especially in the case of thicker shields.

The transformer linearity coefficient as a function of the frequency of the input primary signal is shown in Fig. 11. The input signal on the primary coil is present, but without the external disturbance. Observe that both shields have a similar behavior, but the linearity coefficient is not a constant value as desired. The results from both Figs. 10 and 11 were performed for the cylindrical shield shape with R=38 mm and H=2R.

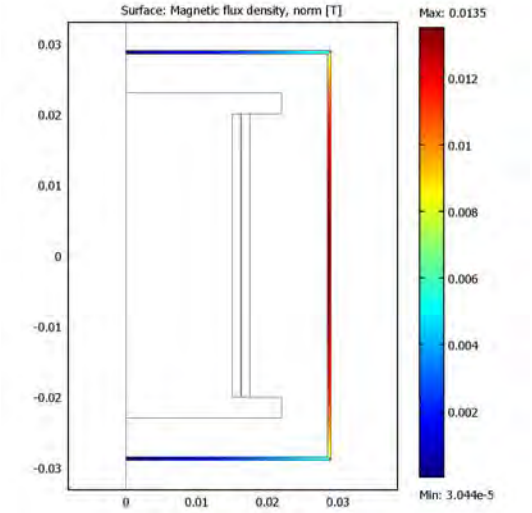

Figure 12. Magnetic flux density along the shield of the thickness d=0.5 mm.

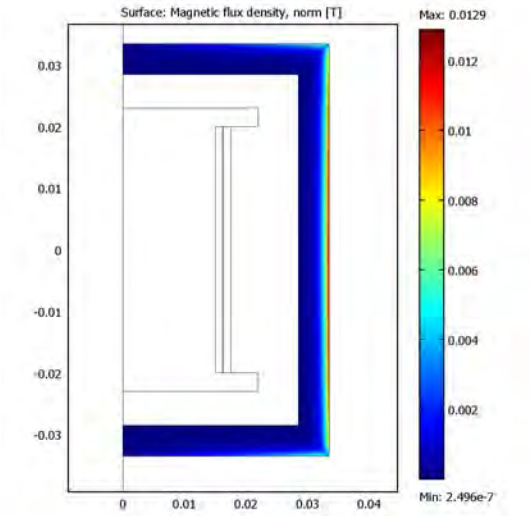

Figure 13. Magnetic flux density along the shield of the thickness d=5 mm.

Distribution of magnetic flux density along the shield, due to external time harmonic magnetic disturbance of 50Hz, is presented in Figs. 12 and 13 for the thicknesses equal to 0.5mm and 5 mm.

7. Conclusions

COMSOL Multiphysics is a very useful FEM based program for a wide range of applications. In this paper, the parameterized probe model was created and used for a large number of simulations in order to find appropriate solution of this particular task.

Some results calculated for the model were well matching with the theoretical results. From the discussed range of the shields, the spherical shields performed best, as expected from theory. However, without COMSOL it would be imposible to conclude what shield shapes and sizes are most appropriate. A cylinder of particular dimensions can be a sufficiently good solution. Future work will employ an optimization technique together with an appropriate fitness function introduced into COMSOL and used for the optimum search.

8. References

[1] IEC 61000-4-7, Testing and measurement techniques– General guide on harmonics and interharmonics measurements and instrumentation, for power supply systems and equipment connected thereto

[2] IEC 61000-3-2 (2001-10) Consolidated Edition. Electro-magnetic compatibility (EMC) – Part 3-2: Limits - Limits for harmonic current emissions (equipment input current <= 16A per phase)

[3] B. Vujičić, D. Herceg, I. Župunski, Merenje zašumljenih signala stohastičkom metodom, 51. Konferencija ETRAN Herceg Novi – Igalo, 2007.

[4] D. Herceg, B. Vujičić, M Prša: Determination of EM field and induced EMF of Voltage Measuring Transformer, 8th International Conference on Applied Electromagnetics PES 2007, Niš, Serbia, 3-5 Sept. 2007.

[5] L. Hasselgren and J. Luomi, Geometrical aspects of magnetic shielding at extremely low frequency. IEEE Trans. EMC 37 3 (1995), pp. 409–420.

[6] BS EN 61000-4-8:2010 Electromagnetic compatibility (EMC). Testing and measurement techniques. Power frequency magnetic field immunity test.

[7] H. Kaden, Wirbelstrome und Schirmung in der Nachrich-tentechnik, Springer, Berlin, pp. 78-91, 1959.

9. Acknowledgements

This paper is a part of the two projects no. 11024 and 18043, supported by the Ministry of Science and Technological Development, Republic of Serbia. The author is also grateful to DAAD and TU Ilmenay for the continuing support.